

## **Supplementary Information for:**

### **Regions of Focal DNA Hypermethylation and Long-Range Hypomethylation in Colorectal Cancer Coincide with Nuclear Lamina-associated Domains**

Benjamin P. Berman<sup>1</sup>, Daniel J. Weisenberger<sup>1</sup>, Joseph F. Aman<sup>1</sup>, Toshinori Hinoue<sup>1</sup>, Zachary Ramjan<sup>1</sup>, Yaping Liu<sup>1</sup>, Houtan Noushmehr<sup>1</sup>, Christopher P.E. Lange<sup>2,3</sup>, Cornelis M. van Dijk<sup>4</sup>, Rob A.E.M. Tollenaar<sup>3</sup>, David Van Den Berg<sup>1</sup>, Peter W. Laird<sup>1\*</sup>

[1] USC Epigenome Center, University of Southern California, Keck School of Medicine, Los Angeles, CA

[2] Department of Surgery, Groene Hart Hospital, Gouda, The Netherlands

[3] Department of Surgery, Leiden University Medical Center, The Netherlands

[4] Department of Pathology, Groene Hart Hospital, Gouda, The Netherlands

\* To whom correspondence should be addressed. Email: [plaird@usc.edu](mailto:plaird@usc.edu)

Phone: (323) 442-7890, FAX: (323) 442-7880.

Keywords: DNA methylation, epigenome, methylome, colorectal cancer, whole genome bisulfite sequencing, nuclear lamina, gene silencing, replication timing

Abbreviations: hESCs (human Embryonic Stem Cells), iPSCs (induced Pluripotent Stem Cells), MR (Methylation-Resistant), MP (Methylation-Prone), ML (Methylation Loss), PMD (Partially Methylated Domain), LAD (Lamina-Associated Domain), CGI (CpG Island), TSS (Transcription Start Site), base pair (bp), kilobase (kb), megabase (Mb)

## Supplementary Note:

### Bisulfite-seq library construction and bisulfite conversion

DNA libraries from each tissue sample were prepared using a customized DNA sample preparation protocol. Sample genomic DNA (5 µg) was fragmented using a S2 ultrasonicator (Covaris, Woburn, MA). Sizing of 50-100 ng fragmented DNA was performed using an Experion automated electrophoresis system and Experion 1K DNA Analysis kit (Bio-Rad, Hercules, CA) to confirm the correct average size and size range expected for each application. Fragmented DNA was repaired to blunt ends using the END-It kit (Epicentre Biotechnologies, Madison, WI). The end-repaired DNA was purified and recovered using a Qiagen MinElute PCR purification column. Addition of an 'A' base to the 3' end of blunt DNA was then accomplished using Klenow exo (3'->5' exonuclease minus) (New England Biolabs, Ipswich, MA). The A-tailed DNA was then purified using the Qiagen MinElute PCR purification columns. Adapters with a 3' 'T' overhang were ligated to the end-modified DNA (see below).

For whole genome bisulfite sequencing, modified Illumina paired-end (PE) adapters were used in which cytosine bases in the adapter are replaced with 5-methylcytosine bases (Integrated DNA Technologies, Coralville, IA) to prevent conversion of the adapter sequence during bisulfite treatment. Double stranded annealed adapters were prepared by annealing and then ligated to the end-repaired DNA samples using ultrapure, rapid T4 ligase (Enzymatics, Beverly, MA) and purified on a Qiagen PCR purification column.

DNA libraries were bisulfite converted with the Zymo EZ DNA Methylation kit (Zymo Research, Orange, CA) according to the manufacturer's specifications. We then performed a series of MethyLight-based, quality control steps to ensure complete

bisulfite conversion as described in the report from Campan and colleagues (PMID: 18987824). Specifically, each bisulfite-converted DNA sample was subject to four MethyLight assays to measure bisulfite conversion completeness and the amount of bisulfite converted DNA from each sample.

Quantitative PCR (qPCR) was performed on a fraction (1 ul) of the Adapter-ligated library using primers from Illumina (PE 1.0/2.0), master mix (Applied Biosystems 2X SYBR Green) and a serial dilution curve of PhiX library DNA as a standard using an ABI 7900HT real-time PCR machine (Applied Biosystems, Foster City, CA). Based on the amplification curve from the qPCR, the optimal cycle number was determined for each library as plateau cycle, where the reaction exits the linear phase of amplification, minus 3 cycles. Amplification of the Adapter-ligated library was performed using *Pfu Cx Turbo Taq Polymerase* (Stratagene, Carlsbad, CA) according to manufacturers instructions and Illumina primers (PE 1.0/2.0). A total of 30% of the bisulfite converted adapter-ligated library was added to a total of 450 ul of reaction mix, vortexed repeatedly, then divided into 9 separate wells (50uL each) for thermal cycling. Following PCR the 9 wells are pooled and PCR products are purified using a QIAquick PCR Purification kit (Qiagen, Valencia, CA). Size fractionation and removal of adapter dimers was performed using 10% TBE acrylamide gels and a 25bp ladder size standard (Invitrogen, Carlsbad, CA). An acrylamide gel slice containing the target library (typically 200-300bp) was excised from the gel, crushed and sheared to break up the acrylamide, soaked in a Tris/Ammonium Acetate buffer (10mM/2.5mM) and precipitated with ethanol. Cluster density was estimated using qPCR with both PhiX library serial dilutions and other libraries previously run with known cluster density. Amplified library

DNA was denatured with NaOH prior to cluster generation. The denatured DNA was diluted to a 4pM concentration.

### **Illumina Genome Analyzer cluster generation and sequencing.**

Attachment of the adapted DNA to the flow cell for Genome Analyzer sequencing was performed on an Illumina Cluster Station fluidics device. We use the Illumina Cluster Generation Kit to prepare each flow cell for sequencing. The protocol was performed for Amplification/Linearization/Blocking on one day and the flow cell is stored in a 50ml conical tube in storage buffer at 4°C for up to two weeks prior to sequencing. Single-end DNA sequencing (76 bp reads) of the bisulfite-converted DNA libraries from the colon tumor and normal adjacent tissues was performed using the Illumina Genome Analyzer Iix as described in <sup>1</sup>.

### **Gene expression assay (Illumina HumanRef-8 v3.0 Expression BeadChip)**

All expression data are available at the NCBI Gene Expression Omnibus (<http://www.ncbi.nlm.nih.gov/geo/>) under accession number GSE25070. Total RNA from 25 normal pairs of colorectal tumor and non-tumor adjacent tissue samples was isolated using the TRIZOL® Reagent (Invitrogen, Burlington, ON) according to the manufacturer's protocol. The concentrations of RNA samples were measured using the NanoDrop 8000 (Thermo Fisher Scientific Inc., Waltham, MA). The quality of the RNA samples was assessed using the Experion RNA StdSens analysis kit (Bio-Rad, Hercules, CA). Expression analysis was performed using the Illumina Ref-8 whole-genome expression BeadChip (HumanRef-8 v3.0, 24,526 transcripts) (Illumina). Briefly,

RNA samples were processed using the Illumina TotalPrep RNA Amplification Kit (Illumina). Total RNA (500ng) from each sample was subject to reverse transcription with an oligo(dT) primer bearing a T7 promoter. The cDNA then underwent second strand synthesis and purification. Biotinylated cRNA was then generated from the double-stranded cDNA template through *in vitro* transcription with T7 RNA polymerase. The biotinylated cRNA (750ng) from each patient was then hybridized to the BeadChips. The hybridized chips were stained and scanned using the Illumina HD BeadArray scanner (Illumina). Scanned image and bead-level data processing were performed using the BeadStudio 3.0.1 software (Illumina). The summarized data for each bead type were then processed using the *lumi* package in Bioconductor. The data were  $\log_2$  transformed and normalized using Robust Spline Normalization (RSN) as implemented in the *lumi* package.

### **CpH methylation**

Recent reports have identified significant DNA methylation occurring in mammalian cells at non-CpG cytosine (CpH) contexts, especially CpA<sup>1-3</sup>. We found that nuclear DNA had slightly greater CpH retention than mitochondrial DNA (0.65% retention vs. 0.25%), suggesting that there is indeed some low level methylation of nuclear CpH DNA. Bisulfite-seq reports of ES and iPSs have indicated that a significant fraction of CpHs are methylated in more than 25% of reads. When we searched for CpHs with >15 reads and at least 25% methylation, we found almost no difference between the normal tumor and colon, and both were at frequencies of approximately 0.1%, a level much more

consistent with that of somatic cell lines than hESCs or iPSCs, which generally had frequencies around 1% (Supplemental Figures S4-S5).

### **Bisulfite-seq identification of focal methylation elements: Methylation-Prone (MP), Methylation-Resistant (MR), and Methylation Loss (ML)**

Unmethylated regions (UMRs) were identified by scanning all windows of at least 10 individual cytosines contained within CpG dinucleotides (each CpG dinucleotide contains two, one on each strand). Only those covered by at least 3 cytosine or thymine reads were counted, and each CpG dinucleotide was assigned a weighting factor defined as the span (in base pairs) between the next CpG dinucleotide upstream and the next CpG dinucleotide downstream. A weighted average was calculated for each window, and those with an average methylation of less than 5% in both tumor and adjacent normal tissue were categorized as methylation resistant (MR). Those with less than 5% in the adjacent normal tissue and greater than 35% in the tumor were characterized as methylation prone (MR), and those with greater than 35% in the adjacent normal tissue and less than 5% in the tumor as methylation loss (ML). Two or more overlapping UMRs of a single class were merged into one. For “clustered” UMR loci, all UMRs of a single class within 500 bp of one another were merged into one.

### **Homer *de novo* motif searches**

*De novo* Motif discovery was performed using HOMER (script v2.6 (10-22-10)), an algorithm previously described<sup>4</sup>. Briefly, MR, MP and ML genomic sequences were extracted using Galaxy<sup>5</sup> and were divided into ‘target’ and ‘background’ sets for each

application of the algorithm (HOMER perl script 'findMotifs.pl'). When MP or MR were classified as 'target', known CpG Islands (CGI) overlapping domains were used for each application. Motifs of length 6, 7, 8, 10, 11, and 12 bp were identified separately for enrichment in 'target' compared to 'background' set using the cumulative hypergeometric distribution to score enrichment. To increase sensitivity of the method, up to two mismatches were allowed in each oligonucleotide sequence and distributions of CpG content in 'target' and 'background' sequences were selectively weighted to equalize the distributions of CpG content in both sets. To identify de novo motifs enriched in MP, 'target' was CGI overlapping MP and 'background' was CGI overlapping MR. To identify de novo motifs enriched in MR, 'target' was CGI overlapping MR and 'background' was CGI overlapping MP. To identify de novo motifs enriched in ML, 'target' was ML and 'background' was MR. Raw outputs from HOMER can be found in Supplementary Materials and Methods. HOMER perl script 'annotatePeaks.pl'<sup>4</sup> and R software plus 'ggplot2' package<sup>6</sup> were used to generate genomic distribution of each identified motifs.

### **Bisulfite-seq identification of Partially Methylated Domains (PMDs) in tumor and IMR90**

Partially methylated domains were identified by scanning all windows of at least 10 kb and containing at least 10 individual cytosines contained within CpG dinucleotides (each CpG dinucleotide contains two, one on each strand). Only those covered by at least 3 cytosine or thymine reads were counted, and each CpG dinucleotide was assigned a weighting factor defined as the span (in base pairs) between the next CpG dinucleotide

upstream and the next CpG dinucleotide downstream. A weighted average was calculated for each window, and those with an average methylation between 20-60% were categorized as partially methylated. All overlapping partially methylated windows were collapsed into a single partially methylated domain (PMD), and those of less than 100 kb in length were discarded.

#### **External data: ENCODE ChIP-seq**

ChIP-seq data was downloaded from the UCSC ENCODE portal (<http://genome.ucsc.edu/ENCODE>). Peaks defined for transcription factor binding clusters were highly specific, but peaks for histone modifications were overly broad so we used only the top 30% of peaks for a given mark, based on the average signal value in the ENCODE peaks files (supplemental fig X).

#### **External data: Hi-C chromatin conformation capture data (GM12678 lymphoblastoid cells)**

We used HiC compartments from GM06990 lymphoblastoid cells taken from<sup>7</sup> (GEO #GSE18199). We downloaded 100 kb bin values based on the first principal component (eigenvector), and removed chromosomes 2 and 10 as the article supplement indicated that those two chromosomes did not follow the A/B compartment structure of the others. We identified compartment boundaries using the definition of two adjacent 100kb windows with negative values, followed by two adjacent windows with positive values (yielding 1,095 boundaries total, see Supplemental Data File).



### **External data: Replication Timing (BJ Fibroblasts)**

We downloaded replication timing data from the supplemental materials of ref<sup>8</sup>. Based on a personal communication with the author Scott Hansen, we calculated the ratio of cells dividing at the late (S4 and G2) time points vs. the early (G1 and S1) timepoints for each locus in the genome, and identified those regions with a late:early log<sub>2</sub>-ratio of greater than 1.5. This cutoff was chosen based on a bimodal distribution of ratios, with a clear peak of early-replicating with values below -1.5, and a clear peak of late-replicating with values above 1.5 (data not shown). We merged any matching positions within 2 kb, and selected those regions larger than 100 kb as late replicating domains (yielding 1,029 late-replicating regions, see Supplemental data file).

## Supplementary Table 1. Bisulfite-seq samples

Sample	ID	PCR cycles	GAllx	Unique mapped reads	Total uniquely mapped sequence (Gb)	Avg coverage	Genome covered	CpH retention (nuclear genome)	CpG retention (nuclear genome)	CpH retention (mitochondrial genome)	CpG retention (mitochondrial genome)	CpGs covered by at least 1 read	CpGs covered by at least 5 non-duplicate reads (either strand)	CpGs covered by at least 10 non-duplicate reads (either strand)	Per cent CpGs filtered out as possible genetic variants
Normal colon mucosa	OTB14838N	5	Single end 75bp	1,205,774,297	86.7	32.22	94.11%	0.61%	73.14%	0.25%	0.25%	87.17%	81.33%	75.74%	2.4%
Colon tumor	OTB14838T	7	Single end 75bp	1,050,881,599	75.8	28.13	94.25%	0.65%	61.98%	0.26%	0.27%	87.09%	79.43%	72.31%	3.8%





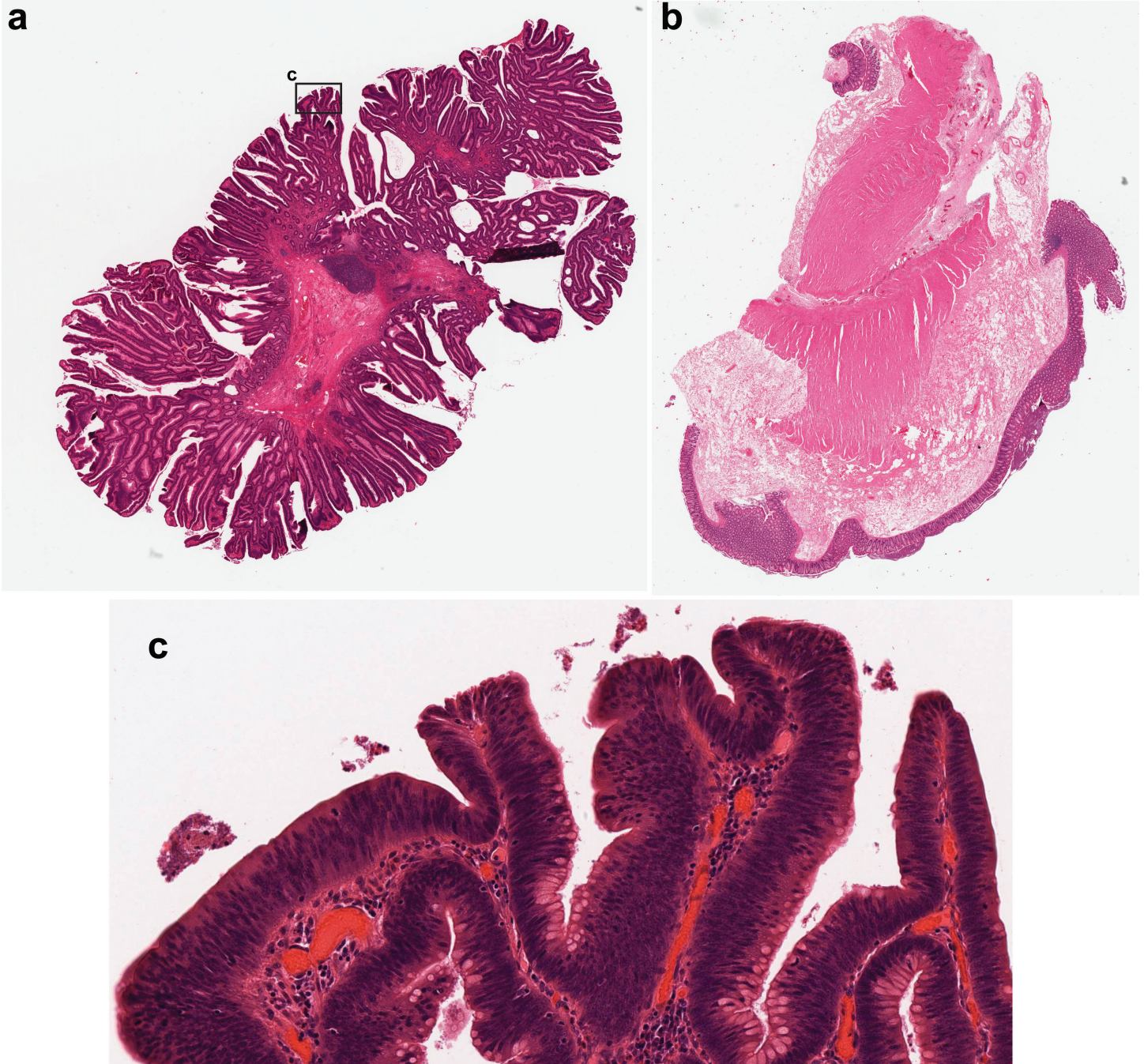




Berman et al., 2011 Supplementary Figure 1

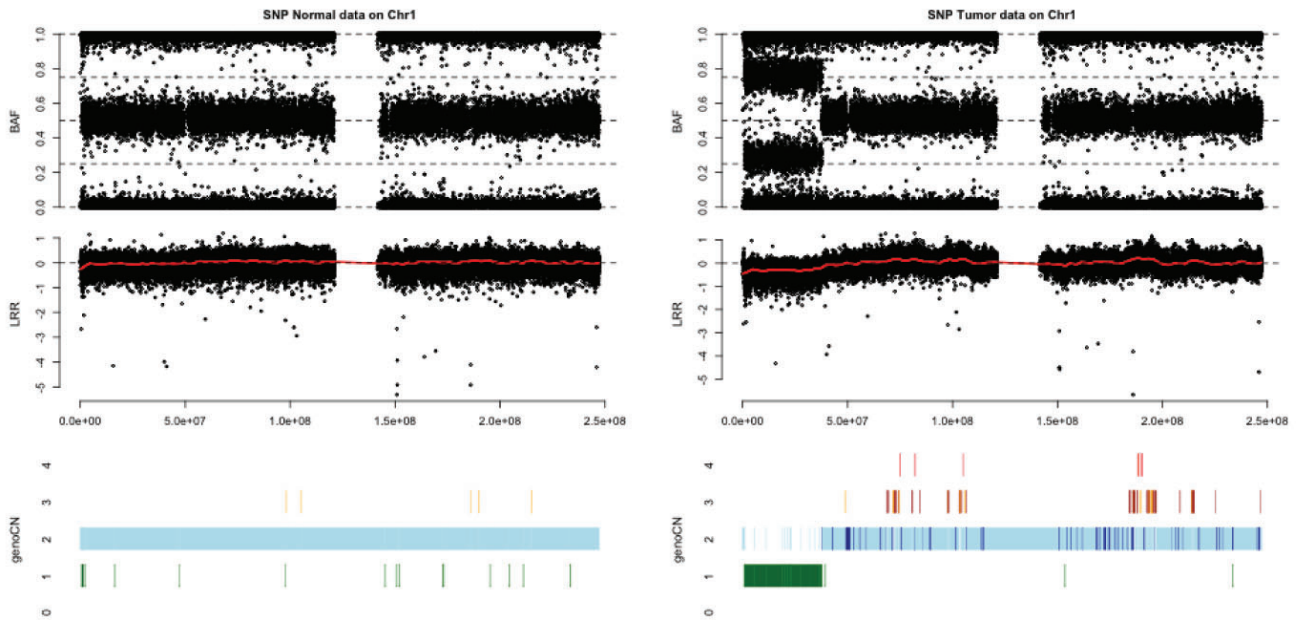
Colon tumor (OTB #B0068109)

Colon mucosa (OTB #B0068110)



**Supplementary figure 1: H&E histological stains show high tumor purity.** Colon tumor (a,c) and normal colonic mucosa (b) images were taken directly from Ontario Tumor Bank. Tumor images show high content of transformed epithelial cells within sample, while colon mucosa primarily consists of normal epithelial nuclei.

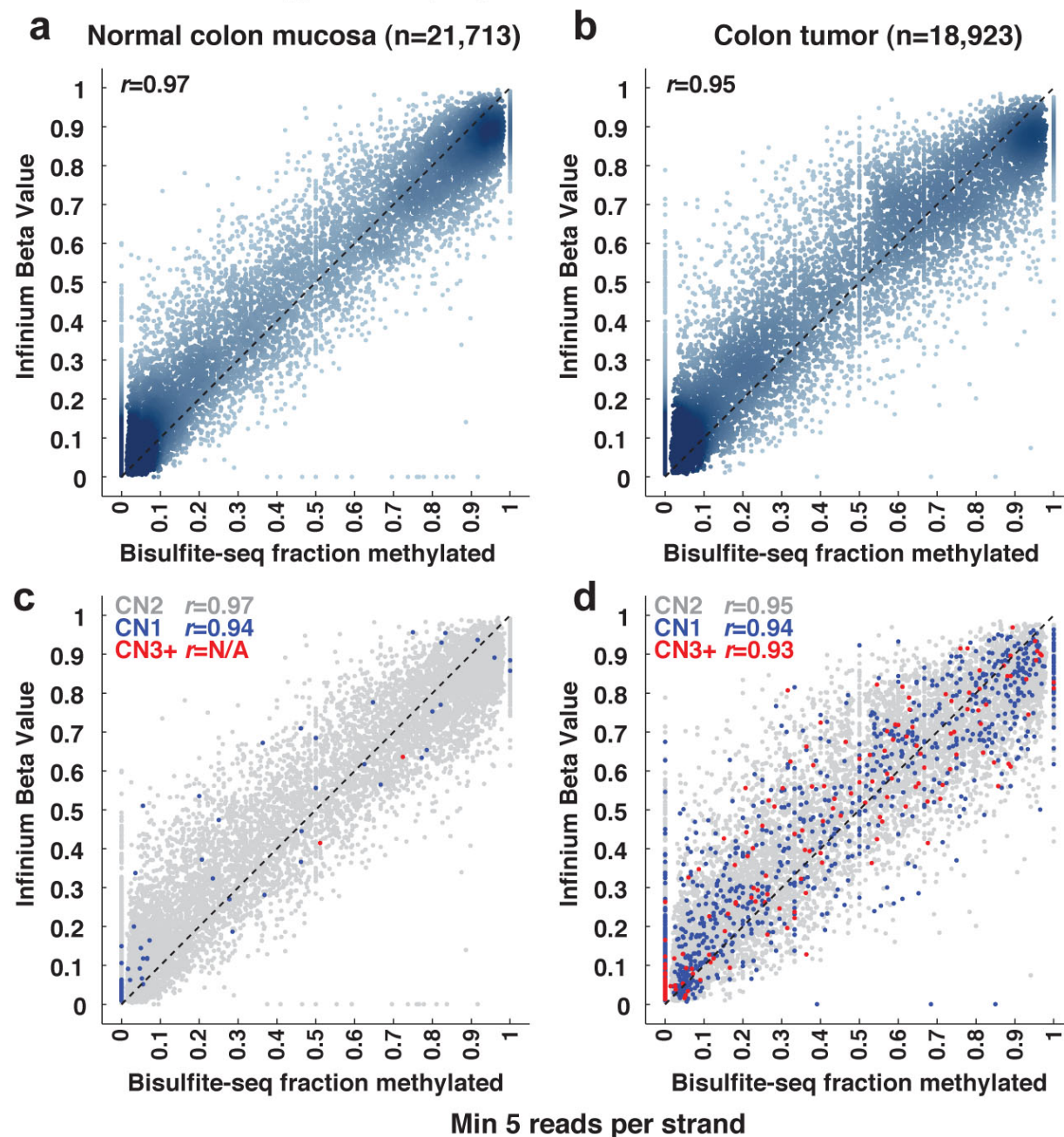
## Berman et al., 2011 Supplementary Figure 2



**Supplementary Figure 2: Copy number alterations identified using the Infinium 1M SNP array.** genoCNV9 plot showing chromosome 1, with a 100 Mbp deletion at the telomeric end of chr1p. Variant copy number calls (genoCN=0, 1, 3, 4) were used to compare Bisulfite-seq and the Infinium DNA methylation values in regions of altered copy number (Supplemental Figure 3).

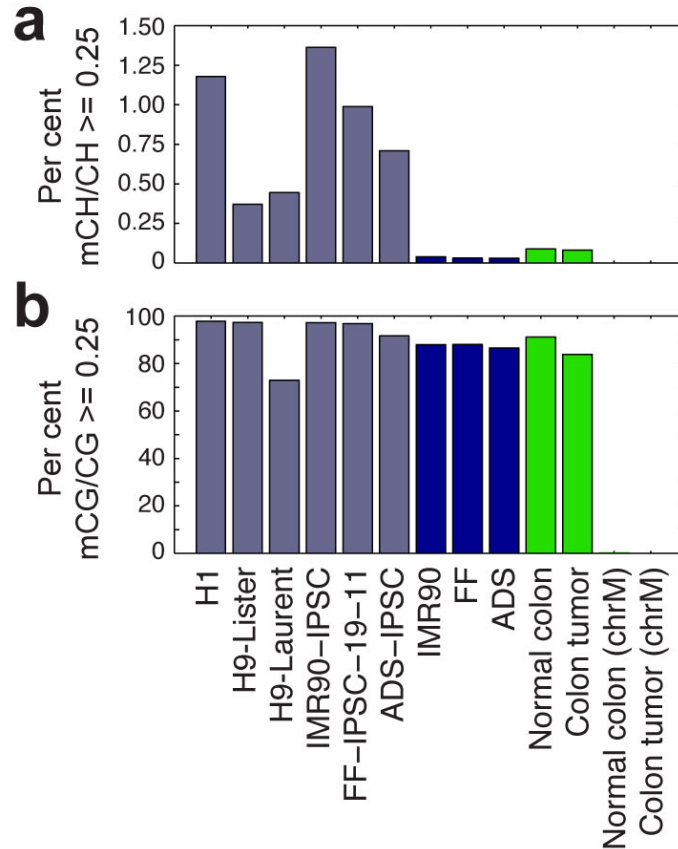
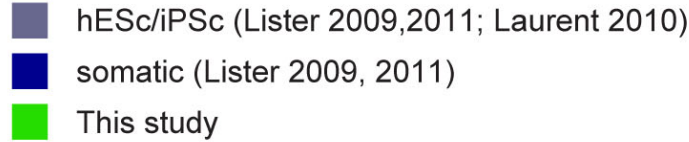


Berman et al., 2011 Supplementary Figure 3



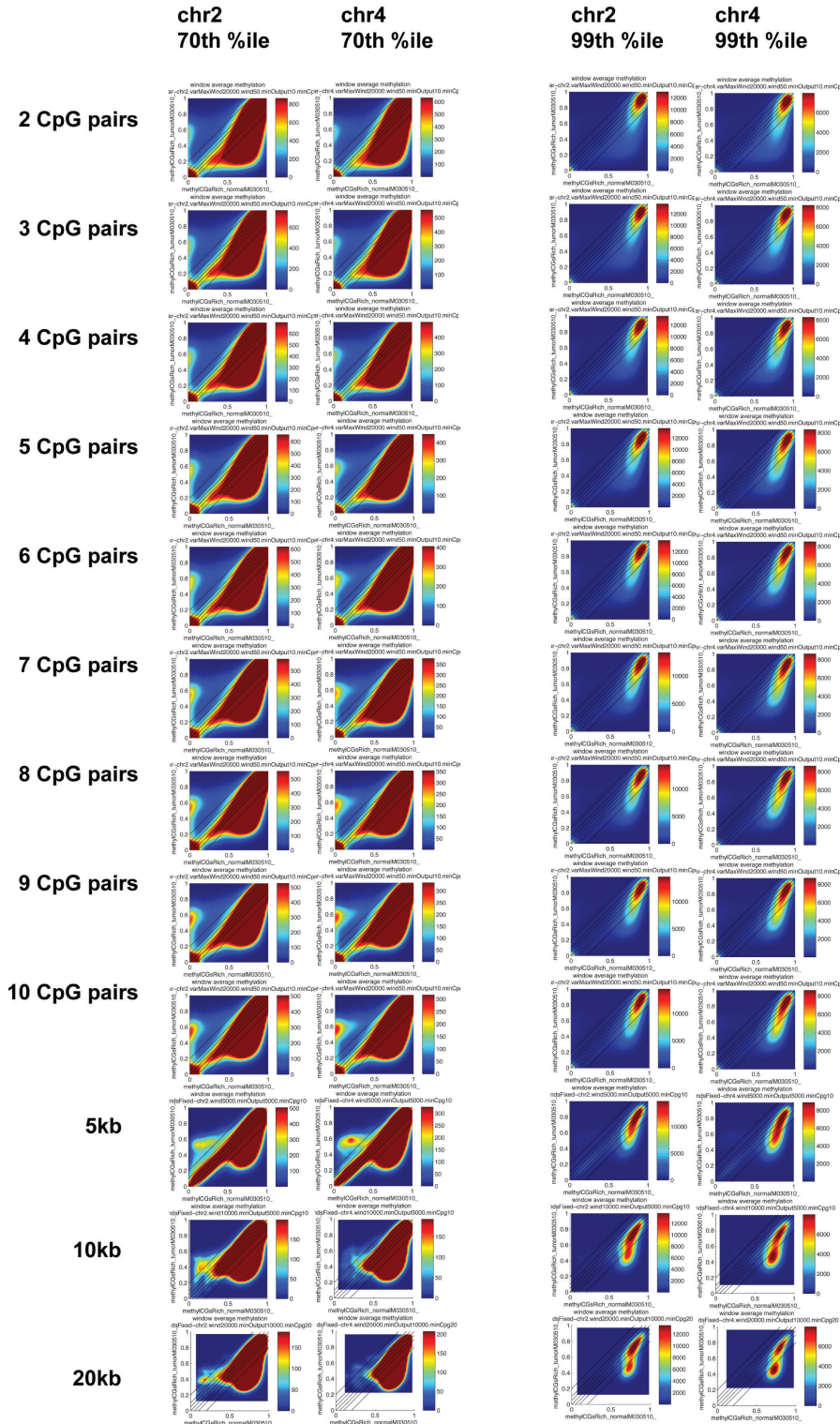
**Supplementary Figure 3: Bisulfite-seq and Infinium methylation array give similar methylation levels, even in regions of altered copy number.** Values are shown for 21,713 CpGs present on Infinium 27k array and with at least 5 reads on each strand of bisulfite-seq data for the normal colon mucosa (a,c), and 18,923 are shown for CpGs with at least 5 reads on each strand of bisulfite-seq data for the colon tumor (b,d). Top panels (a,b) are colored by feature density, while lower panels (c,d) are color-coded by copy number as determined using Infinium 1M SNP array (CN1, copy number loss, CN2 diploid copy number, CN3+ copy number gain).

**Cytosines with 15+ reads,  
Per cent significantly ( $\geq 0.25$ ) methylated**



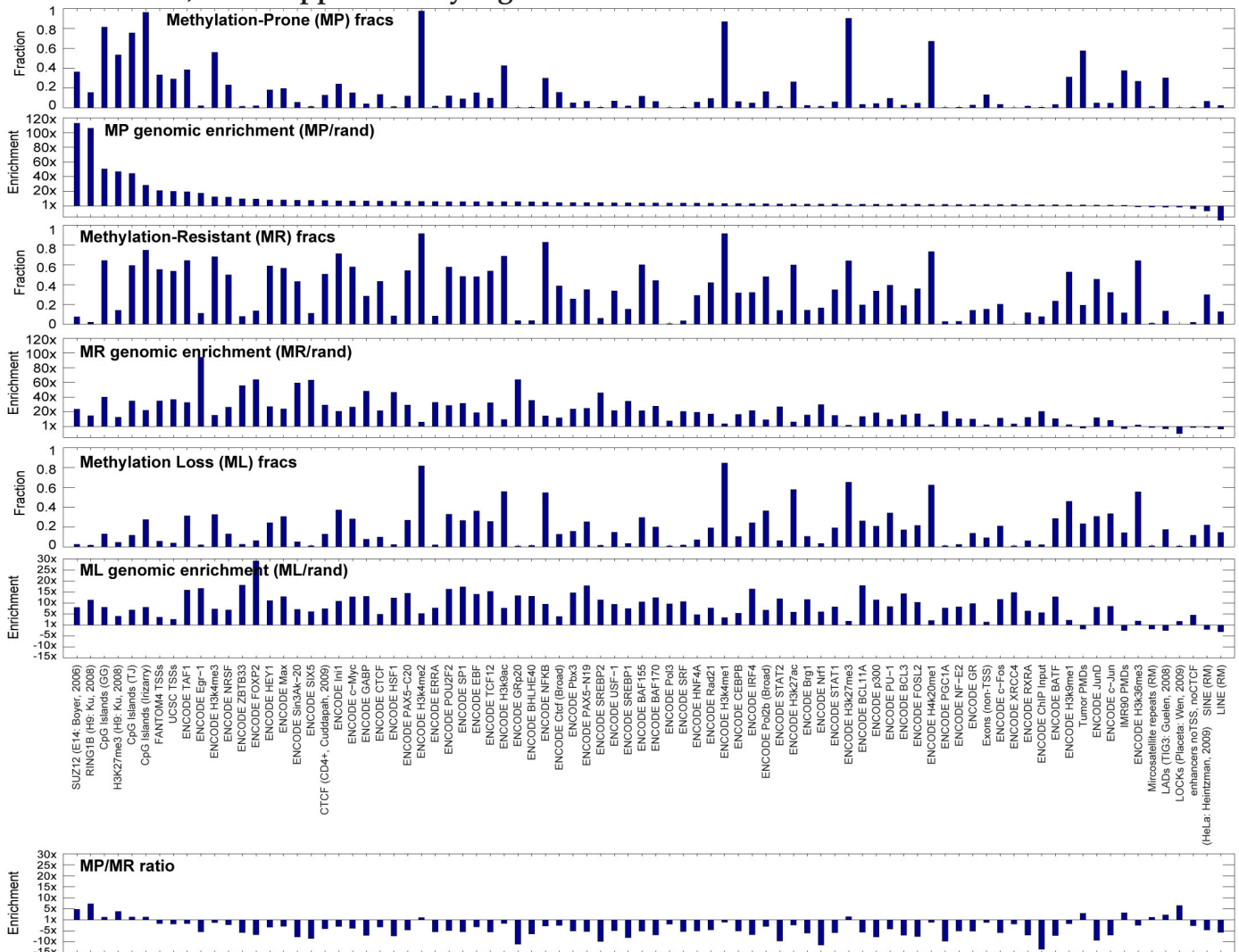
**Supplementary Figure 4: Unlike hESCs, colon tumor and normal mucosa have extremely low levels of CpH methylation.** Normal and colon methylomes (green) were compared to somatic (blue) and hESC/iPSC (gray) cell lines from ref2. Methylation levels were compared at cytosines with at least 15 uniquely positioned reads. Charts show the percentage of cytosines with at least 25% of reads methylated, for CpH (top) and CpG (bottom). For comparison, tumor and normal colon levels were also compared for the mitochondrial genome, which lacks methylation. While the tumor and normal samples do have about 0.1% of nuclear CpHs methylated, significantly more than the mitochondrial genome, this only represents about 30,000 individual CpHs. These levels are similar to those of somatic cell lines from ref2, and only about 10% of CpH levels in hESC/iPSC cells.

# Berman et al., 2011 Supplemental Figure 5



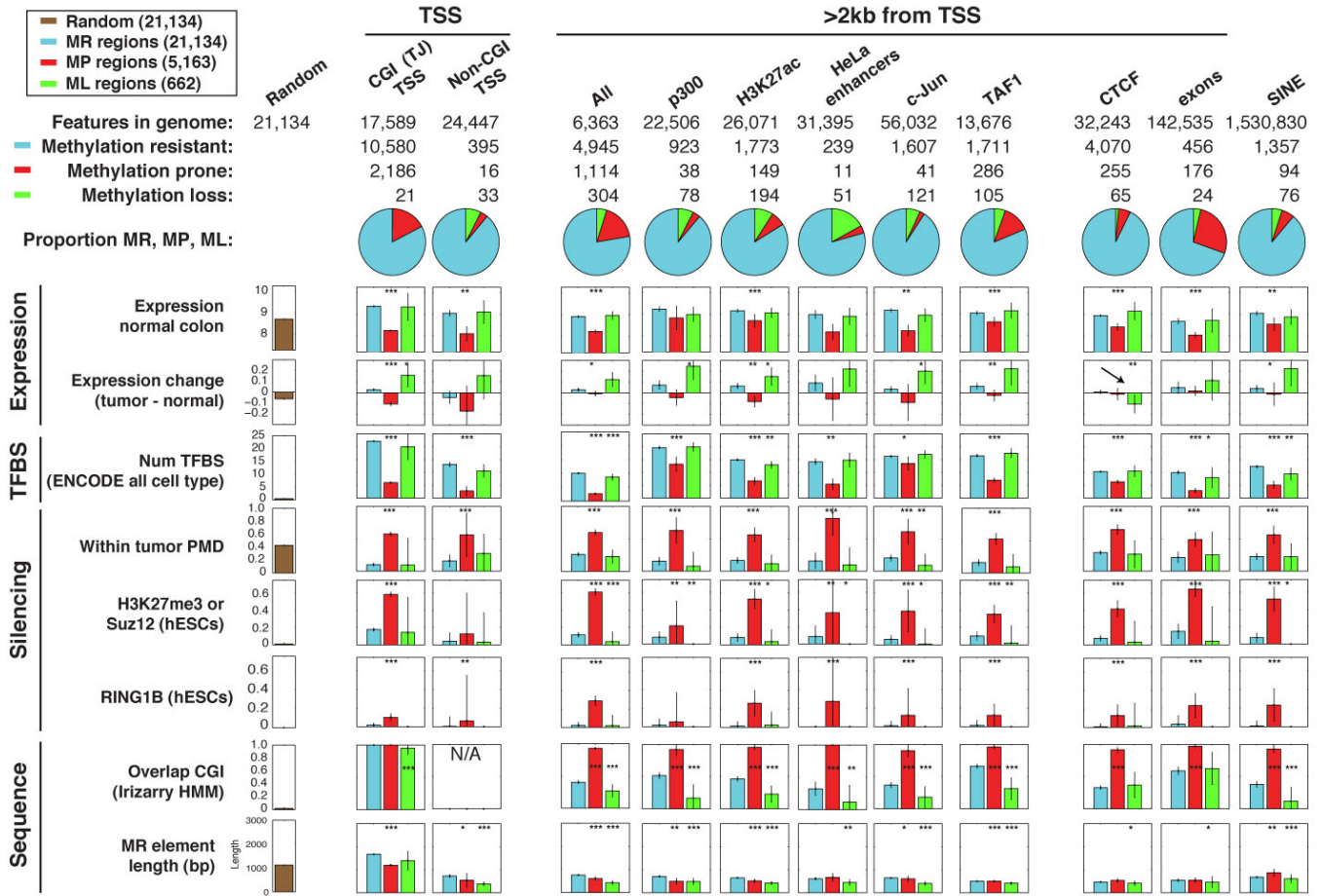
**Supplementary Figure 5: The majority of the tumor and normal colon genomes are methylated. Small genomic windows reveal unmethylated regions in the normal colon, while large genomic windows reveal Partially Methylated Domains in the tumor.** Moving averages of CpG methylation were taken for windows of varying sizes, and joint densities of tumor and normal averages were plotted as scatterclouds (each axis is split into 50 bins of 0.02 methylation units). For each window size, scatterclouds are shown for two different chromosomes (chr2 and chr4), and two different color scales – for the columns labeled “70th %ile”, the darkest red corresponds to the 70th percentile of all 2,500 bin values, and likewise for the 99th percentile. In rows labeled 2-10 CpG pairs, variable window sizes with a minimum number of CpG dinucleotides were used. For rows labeled 5-20 kb, fixed window size were used.

## Berman et al., 2011 Supplementary Figure 6

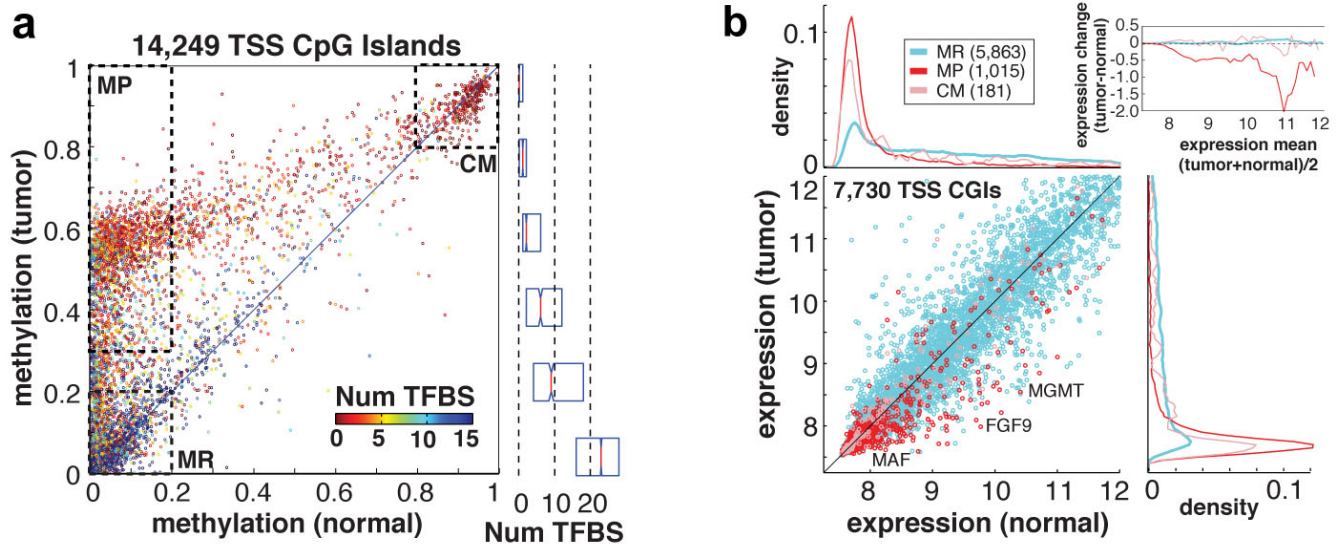


**Supplementary Figure 6: Methylation-Resistant (MR) and Methylation Loss (ML) focal elements are enriched in similar sets of genomic features, distinct from those of Methylation-Prone (MP) elements.** Comparison of each methylation class to ENCODE protein/DNA binding (ChIP-seq) data<sup>10</sup> and other genomic features. “MP frags” plot shows the absolute fraction of MP elements overlapping each feature, while “MP genomic enrichment” was determined by dividing this fraction by the average fraction within ten sets of size-matched, randomly generated genomic locations (shown as fold change). To reduce random variation for features with small numbers of items, a pseudocount of 5 was used to calculate each mean in the ratio. At bottom, the ratio between MP and MR elements is shown, also using a pseudocount of 5.

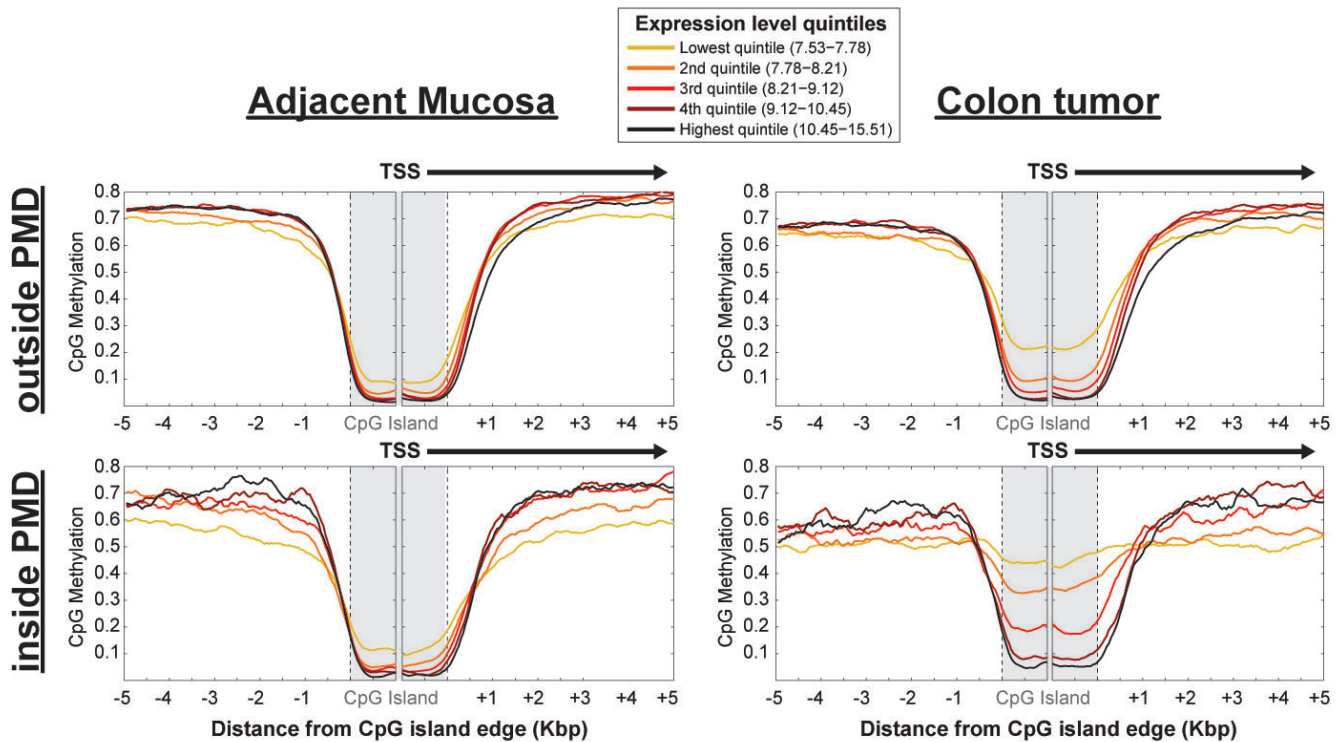
Berman et al., 2011 Supplementary Fig 7



**Supplementary Figure 7: Hypermethylated focal elements are more abundant at promoters than non-coding regulatory sequences, but all have low expression in normal colon, Polycomb Repressive Complex activity, and relative enrichment within PMDs.** Sequence and expression properties are shown for selected classes of MP, MR, and ML elements that either overlap (left) or do not overlap (right) an annotated TSS (from either the UCSC knownGenes or FANTOM411 databases). Each plot shows mean values for the three methylation classes, along with 95% confidence intervals shown as error bars. MP and ML values were each compared to MR values using a two-sided Mann-Whitney U-test, and the significant outcomes were indicated by \*(p<0.05), \*\*(p<0.01), or \*\*\*(p<0.0001).

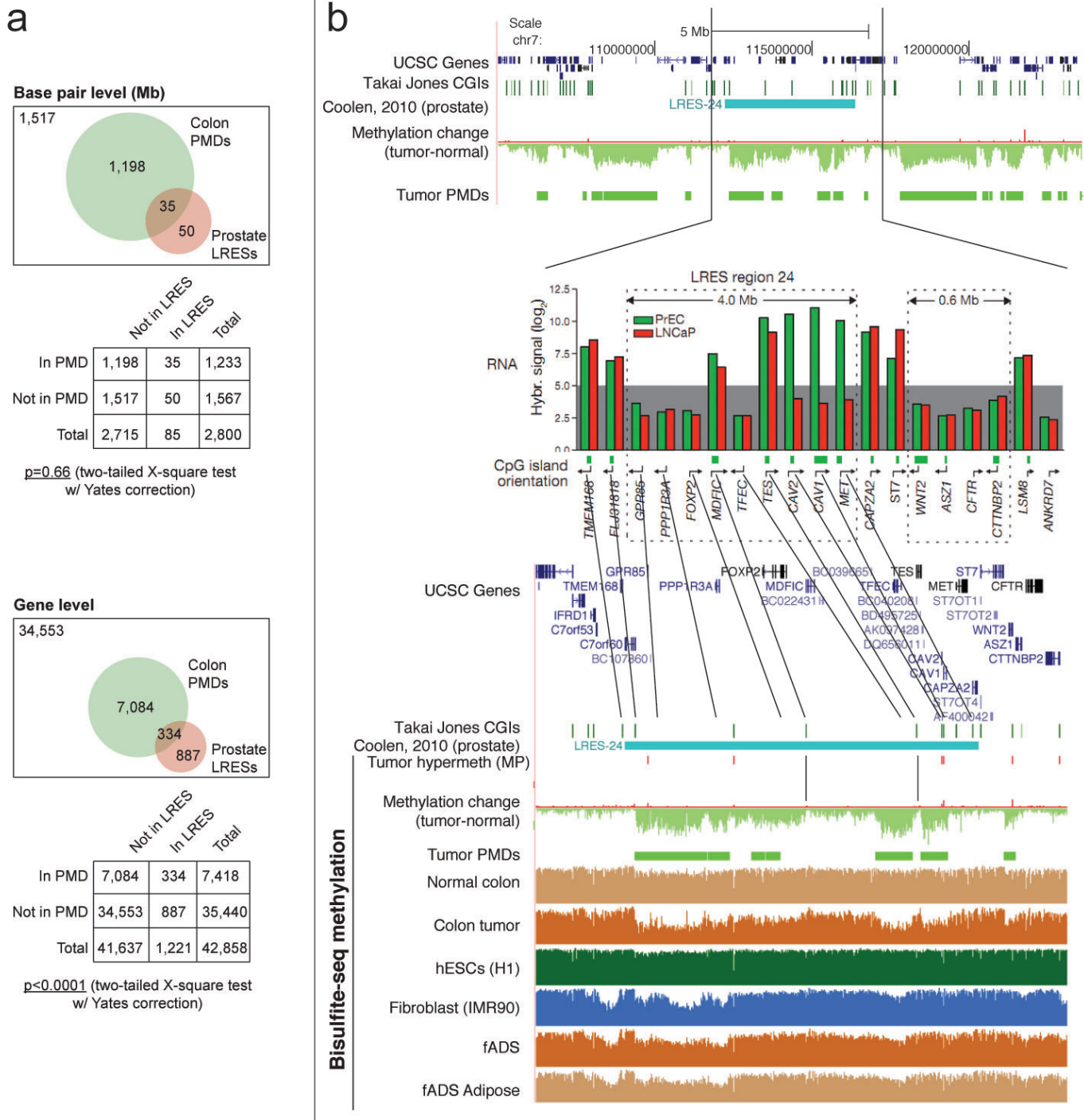


**Supplementary Figure 8: Hypermethylated CpG Island promoters lack transcription factor binding across a number of cell types, and are predominantly unexpressed in normal colon, and are down-regulated in colon tumor.** Mean DNA methylation values for 14,249 Takai-Jones CpG Islands overlapping a transcription start site (TSS) are shown for the colon tumor (y-axis) and the normal-adjacent sample (x-axis). CpG islands were categorized based on their DNA methylation levels - MR - DNA Methylation-Resistant, with methylation < 0.2 for both normal and tumor tissues (n=10,631 loci), MP - DNA Methylation-Prone, with methylation levels < 0.2 in the normal-adjacent tissue and > 0.3 in the tumor sample (n=1,826 loci), CM - constitutively methylated, with methylation > 0.8 in both samples (n=397 loci), and the remainder (n=1,395, labeled “misc”) with intermediate methylation levels. Point color corresponds to the number of ENCODE ChIP-seq transcription factor binding sites (TFBS) from any cell type that overlap the CpG island promoter. **b** Mean log<sub>2</sub>-transformed microarray expression levels for two technical replicates of normal-adjacent colon and colon tumor RNA, showing all genes corresponding to a CpG Island TSSs from panel (a). Each axis shows the expression density plots for each of the three DNA methylation classes. The majority of MP and CM genes having low expression in both tissues. Inset (MA-plot) shows expression change in each methylation class as a function of mean expression in both tissues (using a moving average of 0.1 expression units).



**Supplementary Figure 9: Promoters for most genes with low expression become hypermethylated within tumor PMDs, but not the rest of the genome, and focal hypermethylation corresponds to regional hypomethylation both upstream and downstream of these PMD promoters.** 7,153 CpG islands overlapping a promoter with valid microarray expression data were analyzed with respect to DNA methylation and expression. The top two plots show the 5,809 CGI-TSS located outside of tumor PMDs (Partially Methylated Domains from this study), and the bottom two plots show the 1,344 located inside of PMDs. In each plot, genes are stratified by expression level, and methylation levels are shown relative to the edges of the CpG island, with the left edge representing the 5' upstream region and the right edge representing the transcribed region. Methylation was averaged within sliding 150 bp windows in increments of 50 bp.

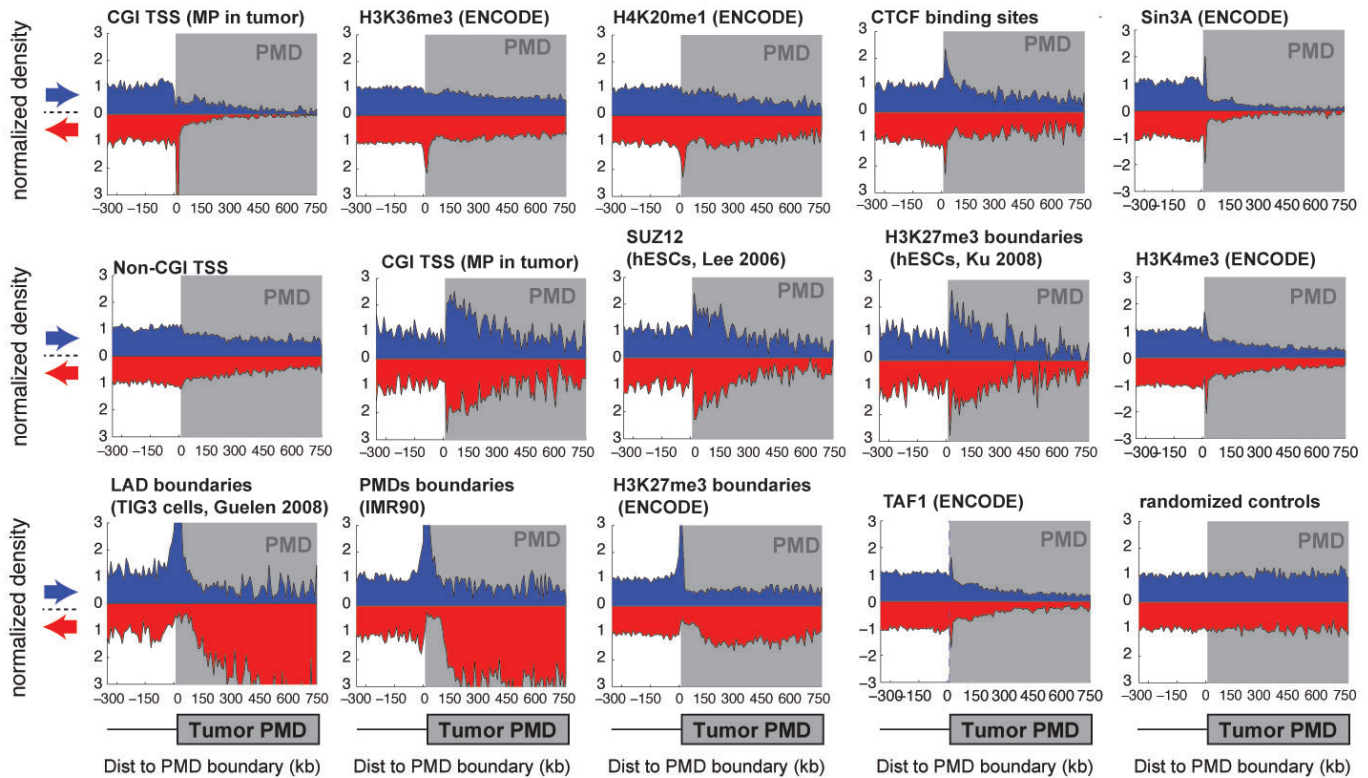
Berman et al., 2011 Supplemental Figure 10



**Supplementary Figure 10: Comparison to domains of Long Range Epigenetic Silencing from prostate cancer<sup>12</sup> shows similarities and differences.** 48 genomic regions from a previous study<sup>12</sup> were compared to 2,850 tumor PMDs identified in the current study. a Overlap at the base pair level is close to random, while genes within Prostate LRESs are significantly enriched for tumor PMD genes ( $p<0.0001$ ). b The region shown in Figure 3 of ref<sup>12</sup> (LRES-24), with methylation tracks from the current study and prostate expression levels from Figure 3 of ref<sup>12</sup>. The top shows that LRES-24 is only one of several colon tumors within the larger genomic region. The bottom shows LRES-24 in greater detail, showing that a large segment in the center of it (from the MFDIC gene to the BC0396651 transcript) is not hypomethylated in the colon tumor. Because MFDIC does not appear to be silenced in LNCaP prostate cancer cells, this region is most likely not part of a true LRES, and is only included in LRES-24 due to the low resolution of the expression array used. Plots for the 7 examples included in ref<sup>12</sup> show this to be the case for a number of LRESs, and are available as a Supplemental Document.

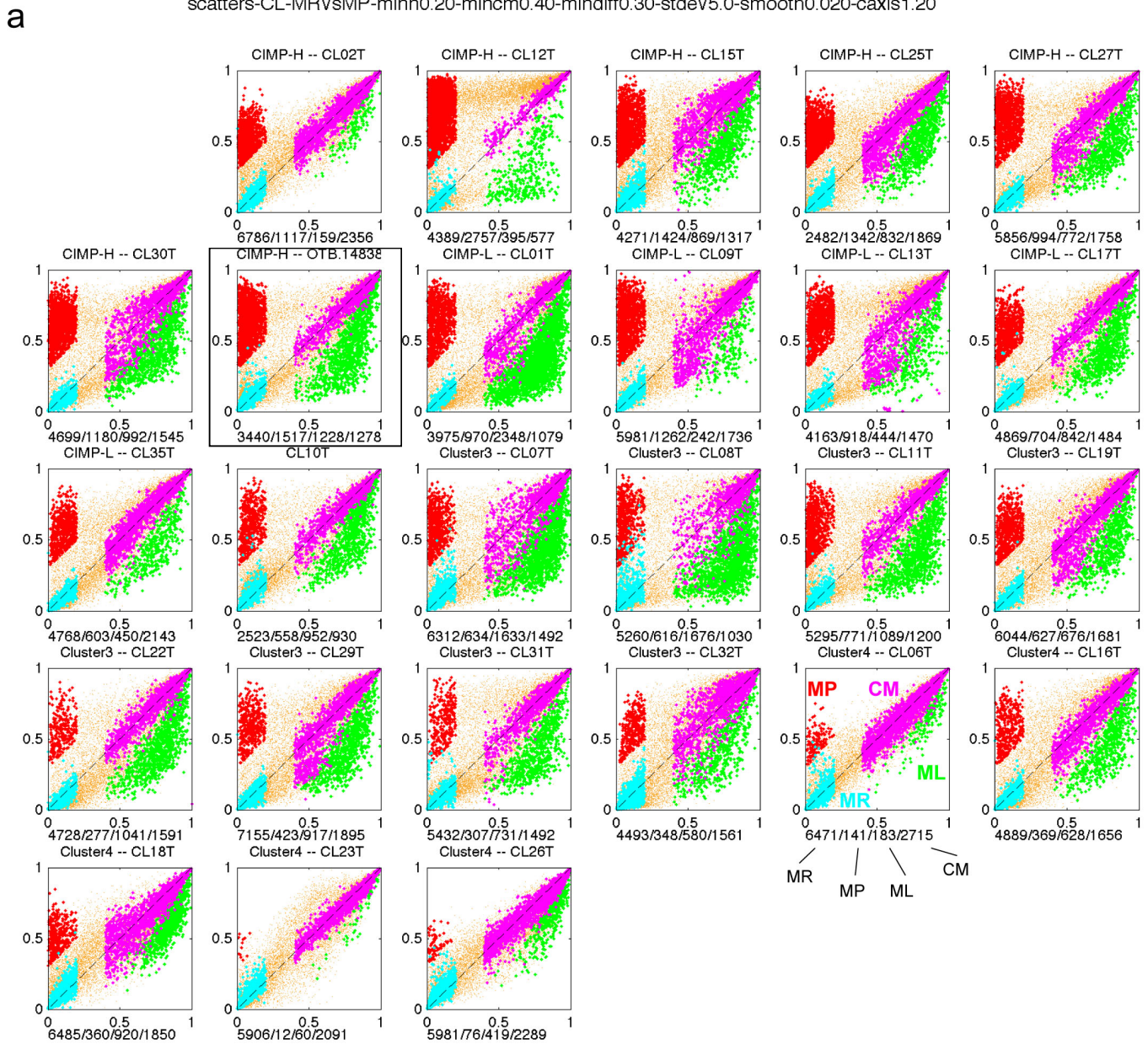


Berman et al., 2011 Supplemental Fig 11



**Supplementary Figure 11: Partially Methylated Domain boundaries suggest a close relationship with nuclear lamina association and Polycomb silencing programs.** Average genomic density of a number of annotation features is plotted for 10 kb bins relative to colon tumor PMD boundaries. Plots are oriented with regions outside the PMD to the left of the midpoint and regions inside the PMD to the right of the midpoint (shaded gray), as shown in the diagrams below each plot. Genomic density was normalized by dividing the value within each bin by the average density within bins lying outside of PMDs. Densities in blue indicate features oriented on the forward strand relative to the PMD boundary (i.e. pointing the same direction as the PMD boundary), and red indicate those oriented on the reverse strand (i.e. pointing the opposite direction).

Berman et al., 2011 Supplemental Figure 12



**Supplementary Figure 12: An independent validation set consisting of 25 colon and rectal tumors and matched normal mucosa shows that the extent of hypermethylation and hypomethylation are correlated within a tumor.** Infinium HumanMethylation27k scatter plots are shown here for colon and rectal tumor/normal pairs used in Figure 6, along with the case used for bisulfite-seq (OTB.14838). They are ordered by methylation subtype from their original study13, “CIMP-H”, “CIMP-L”, “Cluster 3”, and “Cluster 4”. For each pair, four methylation categories (MR, MP, ML, CM) were identified as described in Methods, and array features within each category are shown in a particular color. The number of features in each category is shown below the scatter, as illustrated for “Cluster 4 – CL06T”. OTB.14838 is outlined

# **Supplementary Figure 13**

## **HOMER Results:**












**Methylation-Prone CGI  
promoters (MP-CGIs)**

**vs.**

**Methylation-Resistant CGI  
promoters (MR-CGIs)**

Homer *de novo* Motif Resultsresults for MP CGI promoters  
vs. MR CGI promoters[Known Motif Enrichment Results](#)[Gene Ontology Enrichment Results](#)If Homer is having trouble matching a motif to a known motif, try copy/pasting the matrix file into [STAMP](#)More information on motif finding results: [HOMER](#) | [Description of Results](#) | [Tips](#)

\* - possible false positive

Rank	Motif	P-value	log P-value	Best Match/Details	Motif File
1		1.267e-113	2.600e+02	SeqBias: CA-repeat <a href="#">More Information</a>   <a href="#">Similar Motifs Found</a>	<a href="#">motif file (matrix)</a>
2		7.799e-80	1.822e+02	SeqBias: GA-repeat <a href="#">More Information</a>   <a href="#">Similar Motifs Found</a>	<a href="#">motif file (matrix)</a>
3		6.427e-58	1.317e+02	PB0164.1_Smad3_2 <a href="#">More Information</a>   <a href="#">Similar Motifs Found</a>	<a href="#">motif file (matrix)</a>
4		9.425e-55	1.244e+02	PB0052.1_Plagl1_1 <a href="#">More Information</a>   <a href="#">Similar Motifs Found</a>	<a href="#">motif file (matrix)</a>
5		6.197e-49	1.110e+02	PF0024.1_GGGAGGRR <a href="#">More Information</a>   <a href="#">Similar Motifs Found</a>	<a href="#">motif file (matrix)</a>
6		6.154e-48	1.087e+02	MA0079.2_SP1 <a href="#">More Information</a>   <a href="#">Similar Motifs Found</a>	<a href="#">motif file (matrix)</a>
7		4.624e-47	1.067e+02	PF0099.1_ATCMNTCCGY <a href="#">More Information</a>   <a href="#">Similar Motifs Found</a>	<a href="#">motif file (matrix)</a>
8		9.644e-44	9.905e+01	MA0399.1_SUT1 <a href="#">More Information</a>   <a href="#">Similar Motifs Found</a>	<a href="#">motif file (matrix)</a>
9		4.409e-43	9.753e+01	SeqBias: GCW-triplet <a href="#">More Information</a>   <a href="#">Similar Motifs Found</a>	<a href="#">motif file (matrix)</a>
10		7.393e-42	9.471e+01	YY1/Promoter/Homer <a href="#">More Information</a>   <a href="#">Similar Motifs Found</a>	<a href="#">motif file (matrix)</a>
11		2.503e-36	8.198e+01	PB0206.1_Zic2_2 <a href="#">More Information</a>   <a href="#">Similar Motifs Found</a>	<a href="#">motif file</a>

				<a href="#">Motifs Found</a>	<a href="#">(matrix)</a>
12		1.151e-33	7.584e+01	Sp1/Promoter/Homer <a href="#">More Information</a>   <a href="#">Similar Motifs Found</a>	<a href="#">motif file (matrix)</a>
13		3.673e-30	6.778e+01	CN0218.1_LM218 <a href="#">More Information</a>   <a href="#">Similar Motifs Found</a>	<a href="#">motif file (matrix)</a>
14		3.422e-29	6.554e+01	PB0009.1_E2F3_1 <a href="#">More Information</a>   <a href="#">Similar Motifs Found</a>	<a href="#">motif file (matrix)</a>
15		3.243e-28	6.330e+01	PPARE(DR1)/3T3L1-Pparg-ChIP-Seq/Homer <a href="#">More Information</a>   <a href="#">Similar Motifs Found</a>	<a href="#">motif file (matrix)</a>
16		6.186e-27	6.035e+01	MA0320.1_IME1 <a href="#">More Information</a>   <a href="#">Similar Motifs Found</a>	<a href="#">motif file (matrix)</a>
17		2.267e-20	4.523e+01	PB0203.1_Zfp691_2 <a href="#">More Information</a>   <a href="#">Similar Motifs Found</a>	<a href="#">motif file (matrix)</a>
18		8.133e-17	3.705e+01	MA0205.1_Trl <a href="#">More Information</a>   <a href="#">Similar Motifs Found</a>	<a href="#">motif file (matrix)</a>
19		1.338e-16	3.655e+01	MA0073.1_RREB1 <a href="#">More Information</a>   <a href="#">Similar Motifs Found</a>	<a href="#">motif file (matrix)</a>
20		4.627e-16	3.531e+01	GATA:SCL/Ter119-SCL-ChIP-Seq/Homer <a href="#">More Information</a>   <a href="#">Similar Motifs Found</a>	<a href="#">motif file (matrix)</a>
21		5.860e-14	3.047e+01	CN0146.1_LM146 <a href="#">More Information</a>   <a href="#">Similar Motifs Found</a>	<a href="#">motif file (matrix)</a>
22*		4.551e-12	2.612e+01	CN0177.1_LM177 <a href="#">More Information</a>   <a href="#">Similar Motifs Found</a>	<a href="#">motif file (matrix)</a>

# **Supplementary Figure 14**

## **HOMER Results:**

**Methylation-Resistant CGI  
promoters (MR-CGIs)**

**vs.**

**Methylation-Prone CGI  
promoters (MP-CGIs)**

# Homer *de novo* Motif Results

## Supplementary Figure 14: HOMER results for MR CGI promoters vs. MP CGI promoters













[Known Motif Enrichment Results](#)

[Gene Ontology Enrichment Results](#)

If Homer is having trouble matching a motif to a known motif, try copy/pasting the matrix file into [STAMP](#)

More information on motif finding results: [HOMER](#) | [Description of Results](#) | [Tips](#)

\* - possible false positive

Rank	Motif	P-value	log P-pvalue	Best Match/Details	Motif File
1		3.504e-285	6.550e+02	Sp1/Promoter/Homer <a href="#">More Information</a>   <a href="#">Similar Motifs Found</a>	<a href="#">motif file (matrix)</a>
2		4.433e-197	4.521e+02	NRF1/MCF7-NRF1-ChIP-Seq/Homer <a href="#">More Information</a>   <a href="#">Similar Motifs Found</a>	<a href="#">motif file (matrix)</a>
3		7.761e-193	4.423e+02	PB0007.1_Bhlhb2_1 <a href="#">More Information</a>   <a href="#">Similar Motifs Found</a>	<a href="#">motif file (matrix)</a>
4		9.236e-189	4.330e+02	GABPA/Jurkat-GABPa-ChIP-Seq/Homer <a href="#">More Information</a>   <a href="#">Similar Motifs Found</a>	<a href="#">motif file (matrix)</a>
5		2.773e-175	4.019e+02	PB0020.1_Gabpa_1 <a href="#">More Information</a>   <a href="#">Similar Motifs Found</a>	<a href="#">motif file (matrix)</a>
6		1.472e-135	3.105e+02	YY1/Promoter/Homer <a href="#">More Information</a>   <a href="#">Similar Motifs Found</a>	<a href="#">motif file (matrix)</a>
7		2.107e-122	2.802e+02	MA0043.1_HLF <a href="#">More Information</a>   <a href="#">Similar Motifs Found</a>	<a href="#">motif file (matrix)</a>
8		8.647e-117	2.672e+02	PH0154.1_Prrx1 <a href="#">More Information</a>   <a href="#">Similar Motifs Found</a>	<a href="#">motif file (matrix)</a>
9		1.690e-113	2.597e+02	NFY/Promoter/Homer <a href="#">More Information</a>   <a href="#">Similar Motifs Found</a>	<a href="#">motif file (matrix)</a>
10		5.878e-105	2.400e+02	PH0071.1_Hoxc6 <a href="#">More Information</a>   <a href="#">Similar Motifs Found</a>	<a href="#">motif file (matrix)</a>
11		2.200e-99	2.272e+02	GFY/Promoter/Homer <a href="#">More Information</a>   <a href="#">Similar Motifs Found</a>	<a href="#">motif file (matrix)</a>
12		3.242e-91	2.084e+02	PB0161.1_Rxra_2 <a href="#">More Information</a>   <a href="#">Similar Motifs Found</a>	<a href="#">motif file (matrix)</a>

13		3.380e-85	1.945e+02	PB0016.1_Foxj1_1 <a href="#">More Information</a>   <a href="#">Similar Motifs Found</a>	<a href="#">motif file (matrix)</a>
14		1.810e-82	1.882e+02	PH0174.1_Vax1 <a href="#">More Information</a>   <a href="#">Similar Motifs Found</a>	<a href="#">motif file (matrix)</a>
15		9.761e-82	1.865e+02	PH0117.1_Nkx3-1 <a href="#">More Information</a>   <a href="#">Similar Motifs Found</a>	<a href="#">motif file (matrix)</a>
16		1.397e-81	1.862e+02	PB0182.1_Srf_2 <a href="#">More Information</a>   <a href="#">Similar Motifs Found</a>	<a href="#">motif file (matrix)</a>
17		7.416e-77	1.753e+02	NFAT:AP1/Jurkat-NFATC1-ChIP-Seq/Homer <a href="#">More Information</a>   <a href="#">Similar Motifs Found</a>	<a href="#">motif file (matrix)</a>
18		8.895e-70	1.590e+02	PB0096.1_Zfp187_1 <a href="#">More Information</a>   <a href="#">Similar Motifs Found</a>	<a href="#">motif file (matrix)</a>
19		7.653e-69	1.568e+02	PB0109.1_Bbx_2 <a href="#">More Information</a>   <a href="#">Similar Motifs Found</a>	<a href="#">motif file (matrix)</a>
20		6.485e-65	1.478e+02	PB0109.1_Bbx_2 <a href="#">More Information</a>   <a href="#">Similar Motifs Found</a>	<a href="#">motif file (matrix)</a>
21		7.747e-64	1.453e+02	PH0137.1_Pitx1 <a href="#">More Information</a>   <a href="#">Similar Motifs Found</a>	<a href="#">motif file (matrix)</a>
22		1.127e-52	1.196e+02	CN0230.1_LM230 <a href="#">More Information</a>   <a href="#">Similar Motifs Found</a>	<a href="#">motif file (matrix)</a>
23		4.178e-49	1.114e+02	PB0091.1_Zbtb3_1 <a href="#">More Information</a>   <a href="#">Similar Motifs Found</a>	<a href="#">motif file (matrix)</a>
24		3.107e-45	1.025e+02	PF0151.1_RYAAAKNNNNNNTGW <a href="#">More Information</a>   <a href="#">Similar Motifs Found</a>	<a href="#">motif file (matrix)</a>



# Supplementary Figure 15

## HOMER Results:

Methylation Loss elements  
(ML)

vs.

Methylation-Resistant  
elements (MR)

# Homer *de novo* Motif Results results for ML CGI promoters vs. MR CGI promoters











[Known Motif Enrichment Results](#)

[Gene Ontology Enrichment Results](#)

If Homer is having trouble matching a motif to a known motif, try copy/pasting the matrix file into [STAMP](#)

More information on motif finding results: [HOMER](#) | [Description of Results](#) | [Tips](#)

\* - possible false positive

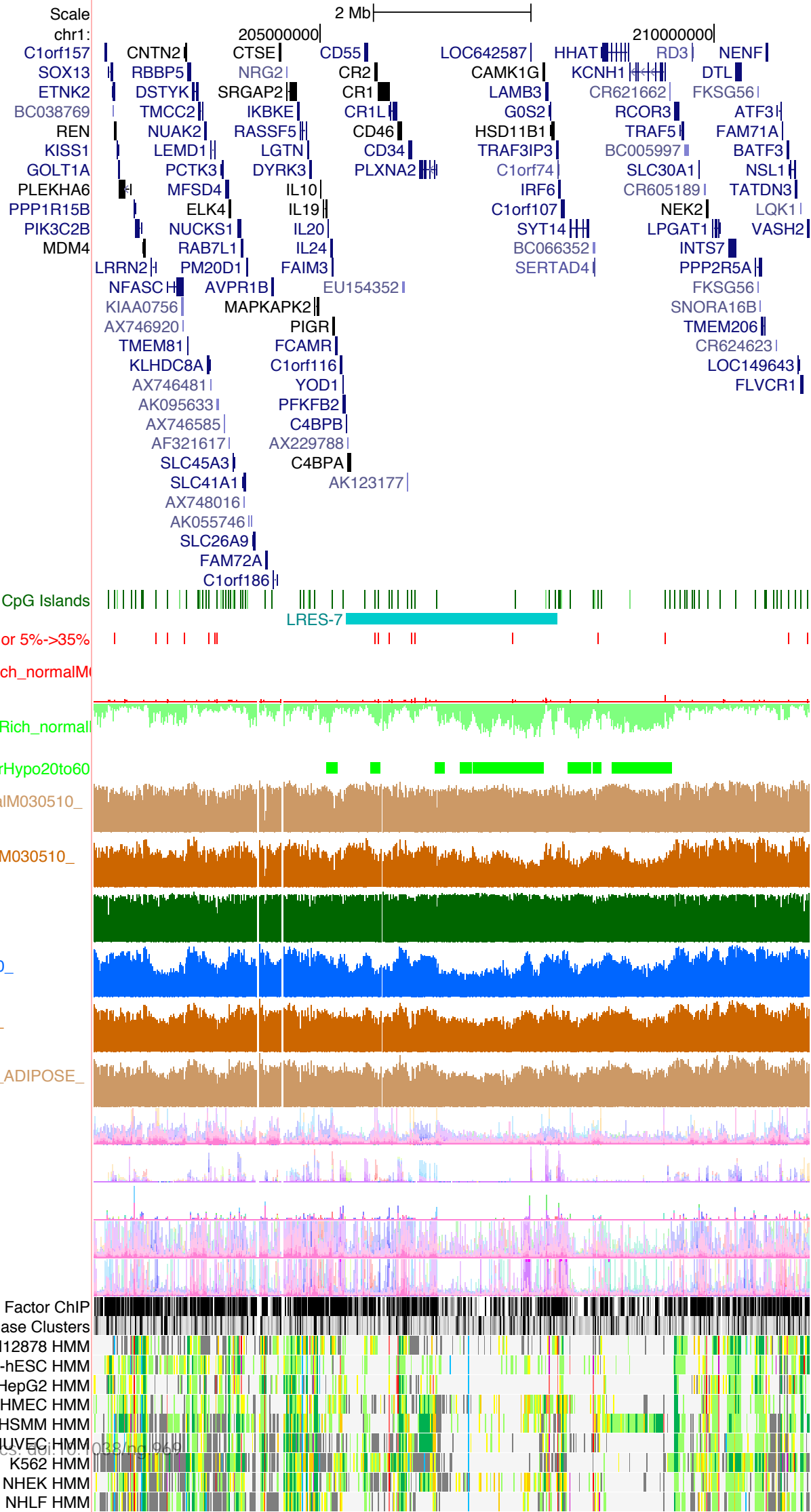
Rank	Motif	P-value	log P-value	Best Match/Details	Motif File
1		2.025e-86	1.973e+02	NFAT:AP1/Jurkat-NFATC1-ChIP-Seq/Homer <a href="#">More Information</a>   <a href="#">Similar Motifs Found</a>	<a href="#">motif file (matrix)</a>
2		5.799e-86	1.963e+02	MA0303.1_GCIN4 <a href="#">More Information</a>   <a href="#">Similar Motifs Found</a>	<a href="#">motif file (matrix)</a>
3		1.575e-47	1.078e+02	MA0345.1_NHP6A <a href="#">More Information</a>   <a href="#">Similar Motifs Found</a>	<a href="#">motif file (matrix)</a>
4		2.177e-41	9.363e+01	PB0116.1_Elf3_2 <a href="#">More Information</a>   <a href="#">Similar Motifs Found</a>	<a href="#">motif file (matrix)</a>
5		6.933e-38	8.556e+01	MA0386.1_TBP <a href="#">More Information</a>   <a href="#">Similar Motifs Found</a>	<a href="#">motif file (matrix)</a>
6		5.176e-20	4.441e+01	PB0120.1_Foxj1_2 <a href="#">More Information</a>   <a href="#">Similar Motifs Found</a>	<a href="#">motif file (matrix)</a>
7		3.888e-19	4.239e+01	MA0346.1_NHP6B <a href="#">More Information</a>   <a href="#">Similar Motifs Found</a>	<a href="#">motif file (matrix)</a>
8		5.040e-19	4.213e+01	PH0148.1_Pou3f3 <a href="#">More Information</a>   <a href="#">Similar Motifs Found</a>	<a href="#">motif file (matrix)</a>
9		5.822e-17	3.738e+01	PH0139.1_Pitx3 <a href="#">More Information</a>   <a href="#">Similar Motifs Found</a>	<a href="#">motif file (matrix)</a>
10		9.258e-		PB0095.1_Zfp161_1 <a href="#">More Information</a>	<a href="#">motif file</a>

		16	3.462e+01	<a href="#">Similar Motifs Found</a> ( <a href="#">matrix</a> )
11		1.702e-15	3.401e+01	CN0106.1_LM106 <a href="#">More Information</a>   <a href="#">Similar Motifs Found</a> <a href="#">motif file</a> ( <a href="#">matrix</a> )
12		1.098e-14	3.214e+01	PB0091.1_Zbtb3_1 <a href="#">More Information</a>   <a href="#">Similar Motifs Found</a> <a href="#">motif file</a> ( <a href="#">matrix</a> )
13		1.343e-14	3.194e+01	MA0088.1_znf143 <a href="#">More Information</a>   <a href="#">Similar Motifs Found</a> <a href="#">motif file</a> ( <a href="#">matrix</a> )
14		1.655e-14	3.173e+01	PB0028.1_Hbp1_1 <a href="#">More Information</a>   <a href="#">Similar Motifs Found</a> <a href="#">motif file</a> ( <a href="#">matrix</a> )
15		1.064e-13	2.987e+01	FOXA1:AR/LNCAP-AR-ChIP-Seq/Homer <a href="#">More Information</a>   <a href="#">Similar Motifs Found</a> <a href="#">motif file</a> ( <a href="#">matrix</a> )
16 *		4.097e-10	2.162e+01	PH0148.1_Pou3f3 <a href="#">More Information</a>   <a href="#">Similar Motifs Found</a> <a href="#">motif file</a> ( <a href="#">matrix</a> )
17 *		4.762e-10	2.147e+01	RUNX(AML)/CD4+-PolII-ChIP-Seq/Homer <a href="#">More Information</a>   <a href="#">Similar Motifs Found</a> <a href="#">motif file</a> ( <a href="#">matrix</a> )

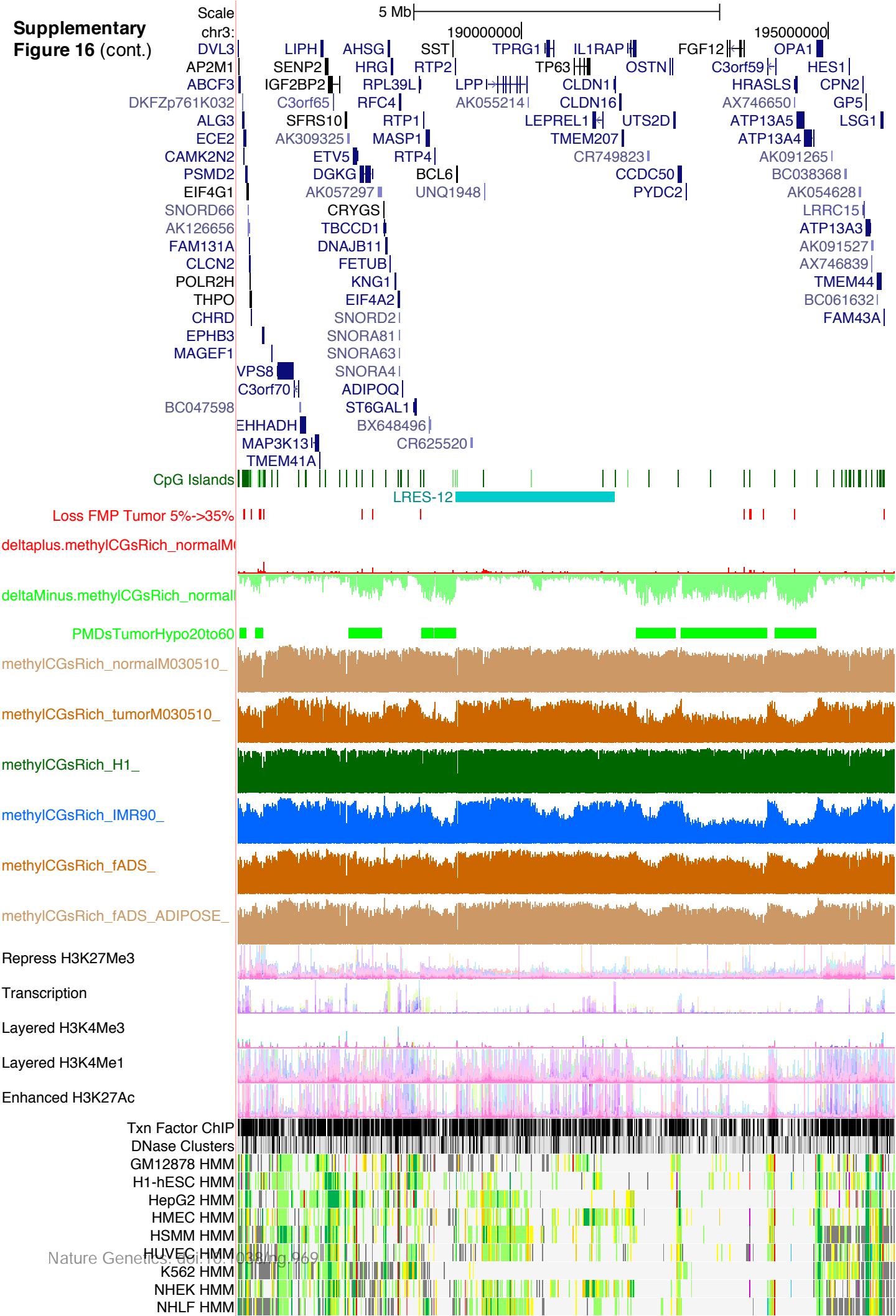
## Supplementary Figure 16

Methylation patterns around prostate cancer Long-Range Epigenetic Silencing (LRES) domains from Coolen, et. al. 2010<sup>12</sup>

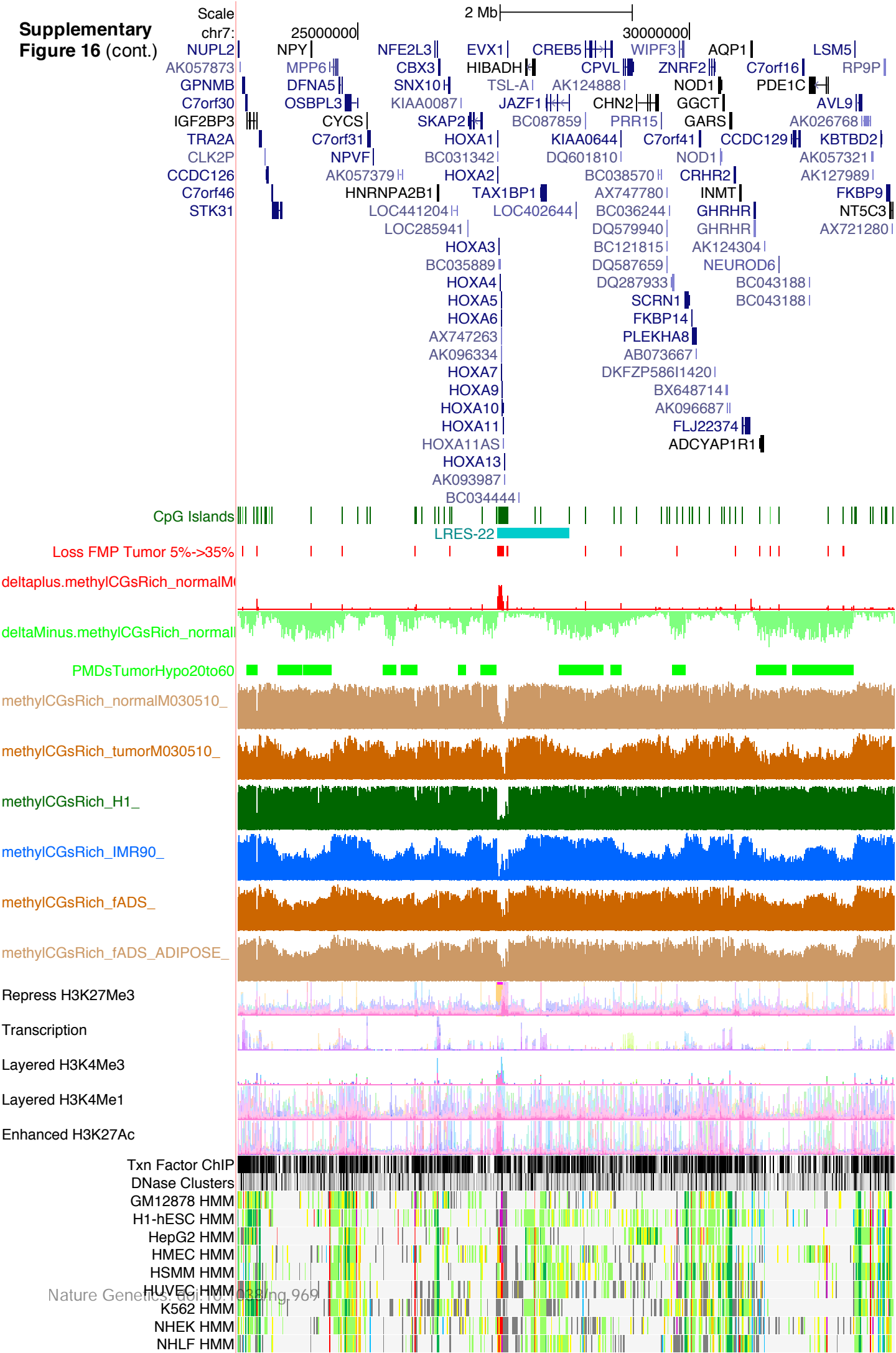
**Supplementary Figure 16 (cont.)**



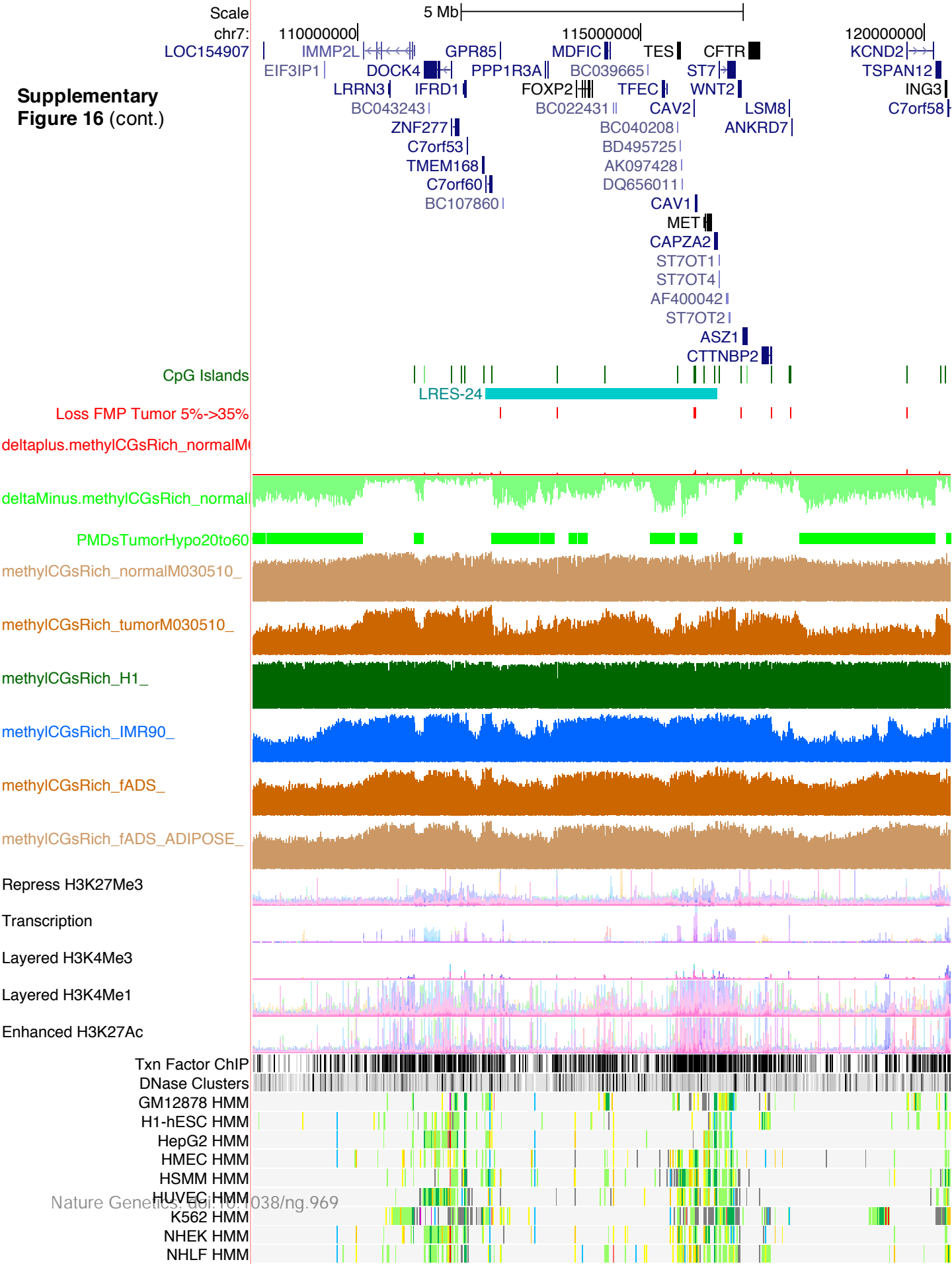
**Supplementary Figure 16 (cont.)**



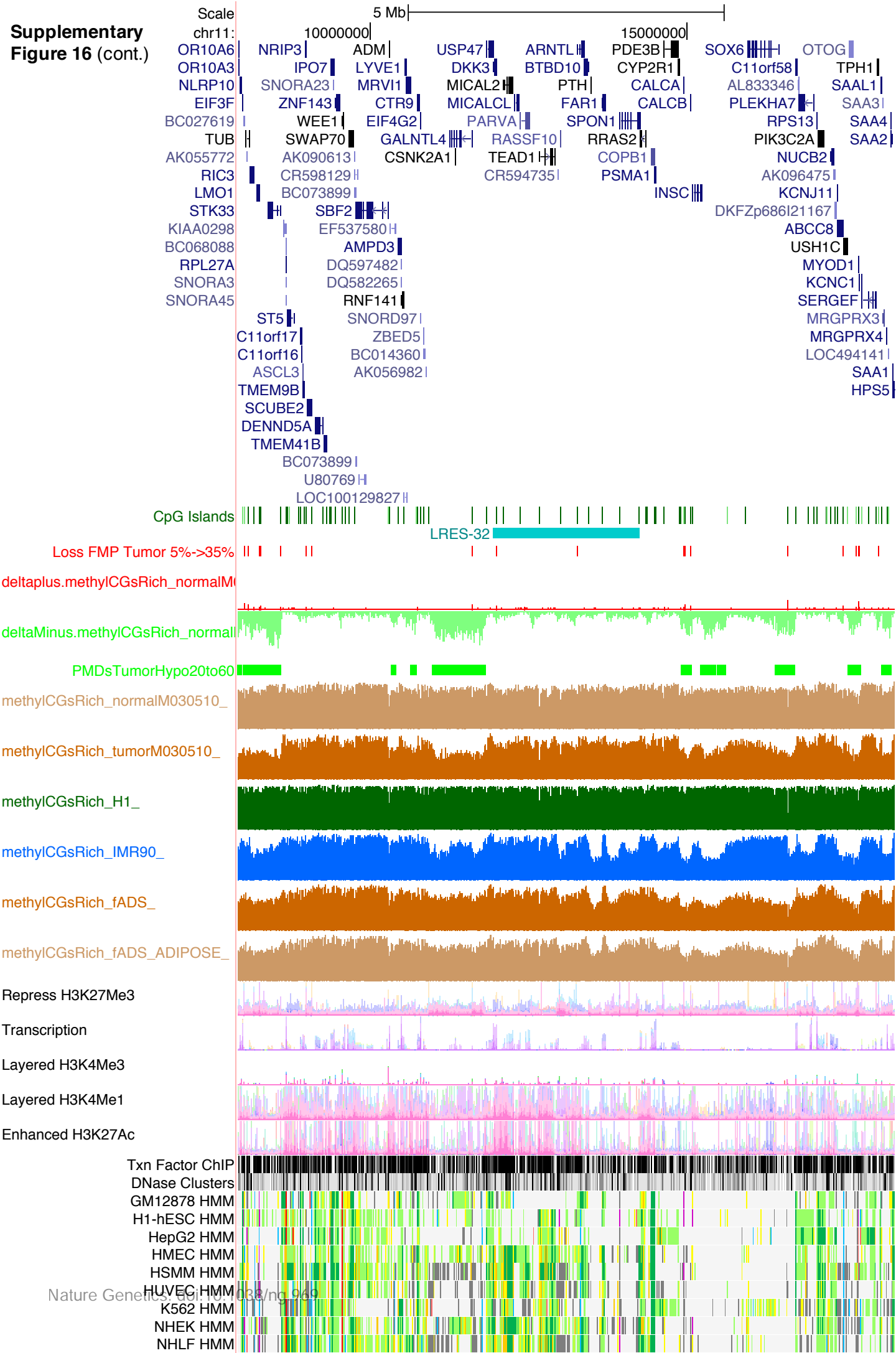
**Supplementary Figure 16 (cont.)**

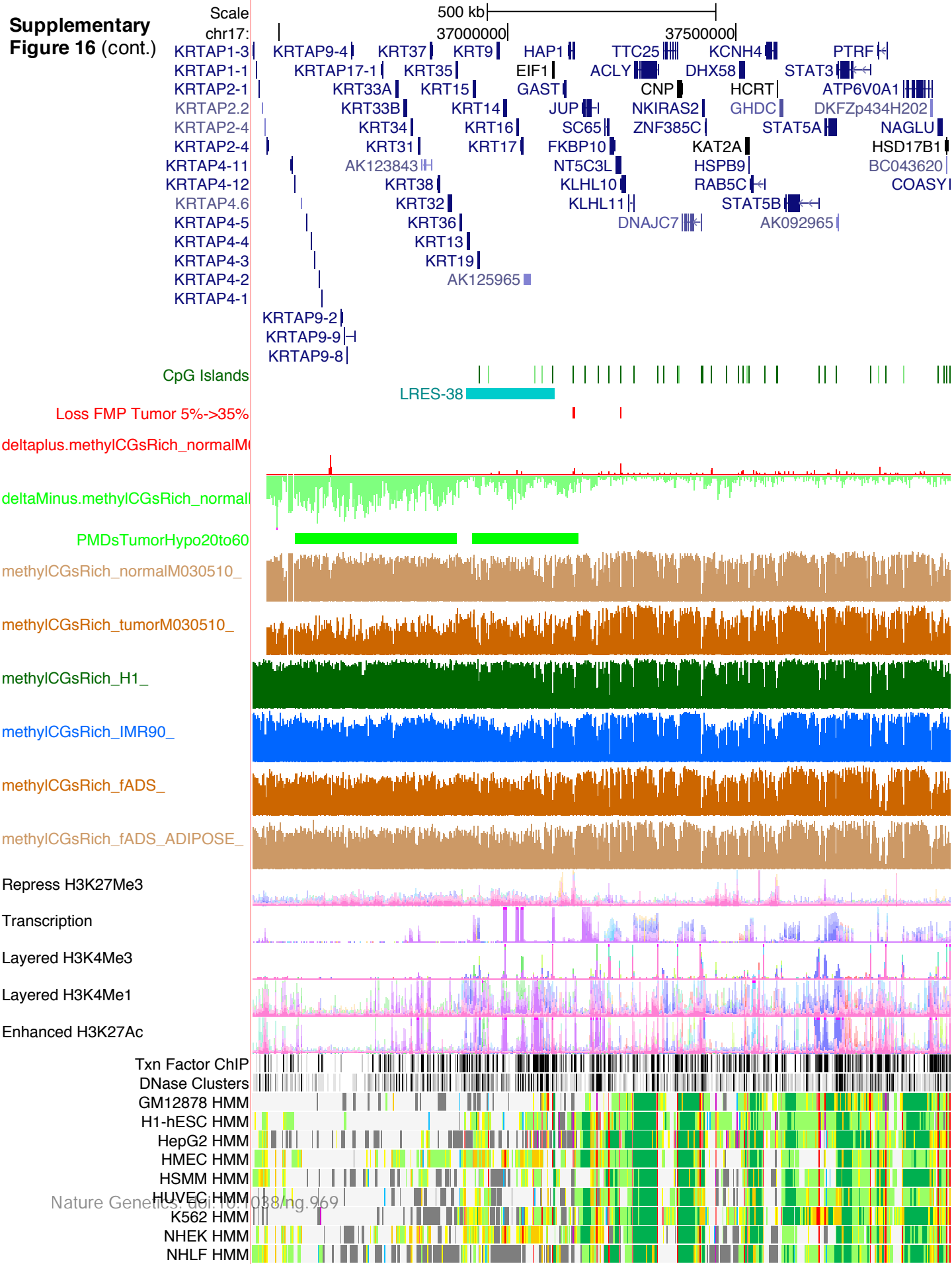


**Supplementary Figure 16 (cont.)**

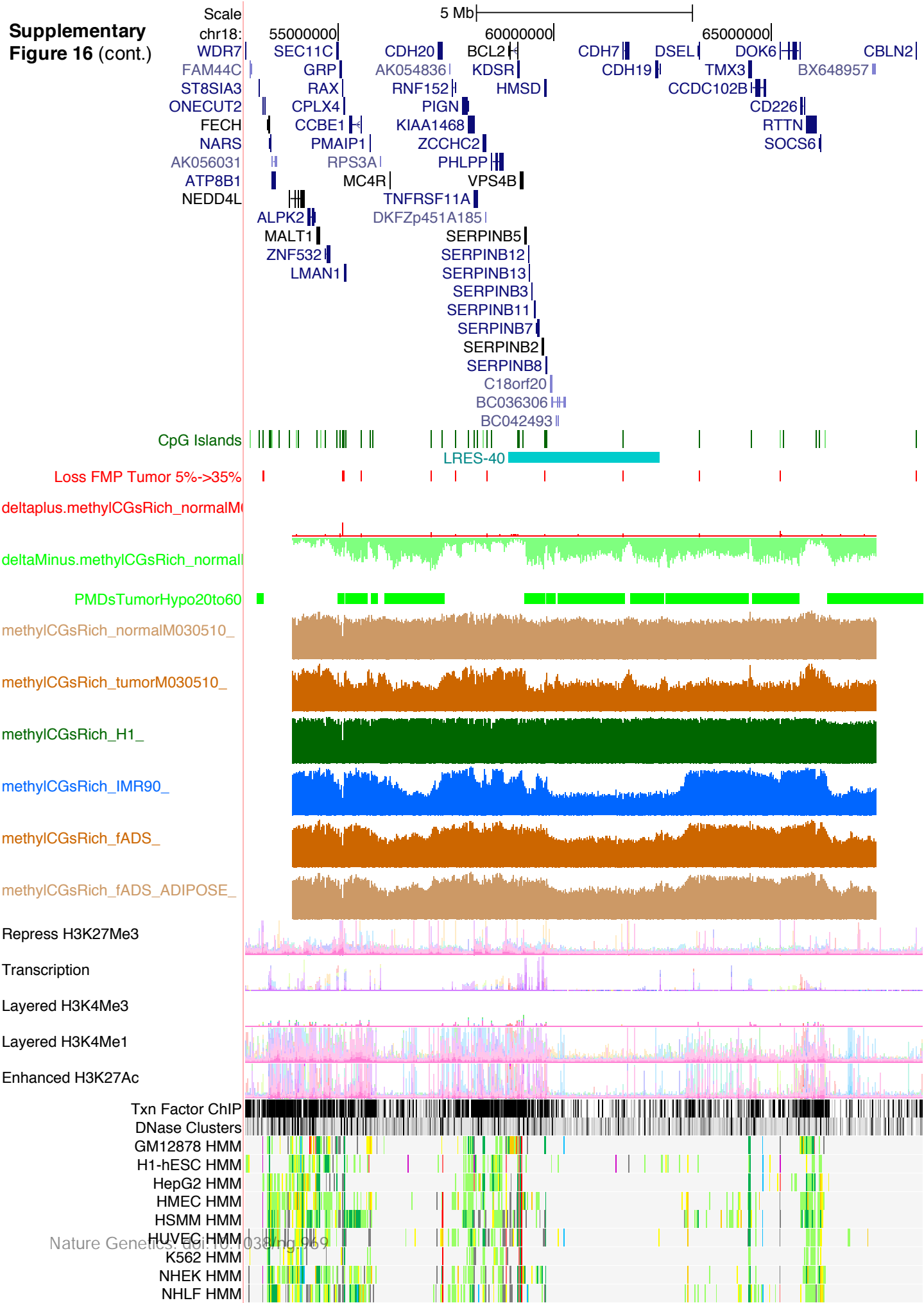








**Supplementary Figure 16 (cont.)**



## References:

1. Lister, R. *et al.* Human DNA methylomes at base resolution show widespread epigenomic differences. *Nature* **462**, 315-322 (2009).
2. Lister, R. *et al.* Hotspots of aberrant epigenomic reprogramming in human induced pluripotent stem cells. *Nature*, 1-8 (2011).
3. Laurent, L. *et al.* Dynamic changes in the human methylome during differentiation. *Genome Res* **20**, 320-31 (2010).
4. Heinz, S. *et al.* Simple combinations of lineage-determining transcription factors prime cis-regulatory elements required for macrophage and B cell identities. *Molecular Cell* **38**, 576-89 (2010).
5. Goecks, J., Nekrutenko, A., Taylor, J. & Team, G. Galaxy: a comprehensive approach for supporting accessible, reproducible, and transparent computational research in the life sciences. *Genome Biology* **11**, - (2010).
6. H., W. *ggplot2: elegant graphics for data analysis*, (Springer, New York, NY, 2009).
7. Lieberman-Aiden, E. *et al.* Comprehensive mapping of long-range interactions reveals folding principles of the human genome. *Science* **326**, 289-93 (2009).
8. Hansen, R.S. *et al.* Sequencing newly replicated DNA reveals widespread plasticity in human replication timing. *Proceedings of the National Academy of Sciences* **107**, 139-144 (2010).
9. Sun, W. *et al.* Integrated study of copy number states and genotype calls using high-density SNP arrays. *Nucleic acids research* **37**, 5365-77 (2009).

10. Consortium, T.E.P. A User's Guide to the Encyclopedia of DNA Elements (ENCODE). *PLoS Biol* **9**, e1001046 (2011).
11. Balwierz, P.J. *et al.* Methods for analyzing deep sequencing expression data: constructing the human and mouse promoterome with deepCAGE data. *Genome Biol* **10**, R79 (2009).
12. Coolen, M.W. *et al.* Consolidation of the cancer genome into domains of repressive chromatin by long-range epigenetic silencing (LRES) reduces transcriptional plasticity. *Nat Cell Biol* **12**, 235-46 (2010).
13. Hinoue, T. *et al.* Genome-Scale Analysis of Aberrant DNA Methylation in Colorectal Cancer. *Genome research* (2011).